

Orientation-Independent Measures of Ground Motion

by David M. Boore, Jennie Watson-Lamprey, and Norman A. Abrahamson

Abstract The geometric mean of the response spectra for two orthogonal horizontal components of motion, commonly used as the response variable in predictions of strong ground motion, depends on the orientation of the sensors as installed in the field. This means that the measure of ground-motion intensity could differ for the same actual ground motion. This dependence on sensor orientation is most pronounced for strongly correlated motion (the extreme example being linearly polarized motion), such as often occurs at periods of 1 sec or longer. We propose two new measures of the geometric mean, GMRotDpp, and GMRotIpp, that are independent of the sensor orientations. Both are based on a set of geometric means computed from the as-recorded orthogonal horizontal motions rotated through all possible non-redundant rotation angles. GMRotDpp is determined as the *p*th percentile of the set of geometric means for a given oscillator period. For example, GMRotD00, GMRotD50, and GMRotD100 correspond to the minimum, median, and maximum values, respectively. The rotations that lead to GMRotDpp depend on period, whereas a single-period-independent rotation is used for GMRotIpp, the angle being chosen to minimize the spread of the rotation-dependent geometric mean (normalized by GMRotDpp) over the usable range of oscillator periods. GMRotI50 is the ground-motion intensity measure being used in the development of new ground-motion prediction equations by the Pacific Earthquake Engineering Center Next Generation Attenuation project.

Comparisons with as-recorded geometric means for a large dataset show that the new measures are systematically larger than the geometric-mean response spectra using the as-recorded values of ground acceleration, but only by a small amount (less than 3%). The theoretical advantage of the new measures is that they remove sensor orientation as a contributor to aleatory uncertainty. Whether the reduction is of practical significance awaits detailed studies of large datasets. A preliminary analysis contained in a companion article by Beyer and Bommer finds that the reduction is small-to-nonexistent for equations based on a wide range of magnitudes and distances. The results of Beyer and Bommer do suggest, however, that there is an increasing reduction as period increases. Whether the reduction increases with other subdivisions of the dataset for which strongly correlated motions might be expected (e.g., pulseline motions close to faults) awaits further analysis.

Introduction

Equations for predicting the ground shaking from earthquakes are usually developed for response spectra corresponding to horizontal shaking. Records of horizontal ground shaking are obtained from orthogonally oriented components, and thus two records are available at each site. There are many ways to use the two horizontal components in ground-motion prediction equations (e.g., Douglas, 2003). In the derivations of several widely used prediction equations these two records are combined into a single measure of shaking intensity by forming the geometric mean of the response spectra for each horizontal component (e.g., Abra-

hamson and Shedlock, 1997), sometimes with a correction of the standard deviation of the predicted motions to approximate a randomly chosen component of ground motion (Boore *et al.*, 1997; Boore, 2005a). One advantage of the geometric mean is that the aleatory uncertainty in ground-motion prediction equations using this measure of ground motion is less than for almost all other measures (Beyer and Bommer, 2006). The geometric mean of the as-recorded motions has one potentially important drawback, however: it is not invariant to the orientation of the sensors. As an extreme case, consider noise-free, linearly polarized ground motion.

If one of the sensors happened to be aligned with the direction of polarization, the response spectrum from the recorded motion on the orthogonal sensor would be zero, and the geometric mean would be zero, regardless of the amplitude of the polarized ground motion. This might be an important consideration close to faults, where rupture directivity and radiation pattern can produce strongly correlated motions, in particular at periods of 1 sec or longer (Spudich *et al.*, 2004). Because obtaining a response spectrum is not a linear operation on a time series (the response spectrum of the sum of two time series is not equal to the sum of the response spectra for each time series), the sensitivity to sensor orientation is also shared by almost all other measures of ground-motion intensity.

Orientation-independent combinations of the two horizontal components have been used in seismology for measures of Fourier spectral amplitudes (e.g., Shoja-Taheri and Bolt, 1977; Lu *et al.*, 1992; Steidl, 1993; Steidl *et al.*, 1996) and Arias intensity (Arias, 1970), but because it is a nonlinear operation, response spectra cannot be derived directly from these “rotary spectra” (to use Gonella’s [1972] term). In this article, we describe new measures of ground-motion intensity that are independent of the as-recorded sensor orientations. These new measures are obtained by computing the geometric means of response spectra for all nonredundant rotations of a given pair of orthogonal, horizontal-component-recorded motions, and then by finding the geometric mean corresponding to a certain percentile of the resulting set of geometric means. We call these new measures “GMRotDpp” and “GMRotIpp”, where “pp” signifies the percentile, most commonly “50.” Using these new measures will remove sensor orientation as a component of aleatory uncertainty, which could be important in probabilistic seismic-hazard calculations of ground motions with very small annual frequencies of exceedance (e.g., Bommer *et al.*, 2004).

Dependence of Geometric-Mean Ground-Motion Intensity on Sensor Orientation: an Illustration

As an illustration of the variability in response spectral amplitude that can occur, depending on the orientation of the orthogonal horizontal sensors, consider the recording of the 1971 San Fernando, California, earthquake obtained at Pacoima Dam. We chose this record for no particular reason, except that it does have a strong pulse in velocity and thus is a good illustration of the problem with the standard way of combining the two components. None of the contributions in this article depend on the use of this one recording. We processed the acceleration time series by applying an acausal low-cut filter with a 0.1-Hz corner frequency. The as-recorded orientations of the horizontal components were 164° and 254°. We show in Figure 1 what the velocity time series would have looked like if the sensors had been oriented in the 242° and 332° or 197° and 287° directions instead (corresponding to rotation angles of 78° and 33°, re-

spectively). These angles were chosen because they give the maximum and the minimum geometric means at a period of 1.0 sec respectively. Note that the maximum geometric mean (time series in left column) corresponds to the velocity pulse being more-or-less equally distributed between the two horizontal components, whereas the minimum geometric mean occurs when the pulse is primarily on one component (time series in right column). The geometric-mean response spectra for various rotations are shown in Figure 2. The spectra for the rotation angles used to give the velocity time series in Figure 1 are shown by the unbroken black lines, and the spectra that used period-dependent rotation angles, chosen to minimize and maximize the geometric means at each oscillator period, are shown with the gray lines. Note that the spectra using the period-independent rotation angle giving a minimum at $T = 1.0$ sec corresponds to the maximum possible geometric-mean response spectrum for periods greater than about 4.0 sec. This means that if the sensors had been placed with an orientation 33° clockwise relative to the actual orientation, the geometric mean would have been the smallest of those from all possible sensor orientations for periods from 0.8 sec to 1.3 sec and the largest possible for periods from 4.0 sec to at least 10 sec. Note also that the ratio of maximum to minimum geometric-mean response spectra is close to 2 for periods near 1 sec and 6 sec. This means that the same ground motion could have given a factor-of-2 difference in the ground-motion intensity measure, depending on the orientation of the sensors as installed in the field.

The sensitivity of the geometric mean to the rotation angle depends on the correlation between components. A simple derivation gives the following equation for the ratio of the geometric mean to the response spectral amplitude on the as-recorded component with the largest response amplitude:

$$GM(\theta)/RS_{\max} = [(1 + \zeta^4)(\cos(\theta)\sin(\theta))^2 + \zeta^2]^{0.25}, \quad (1)$$

where θ is the rotation angle relative to the as-recorded component with the largest response spectrum, and ζ is the ratio of the response spectra from the two as-recorded components (assumed to be statistically independent). This equation is exact when $\zeta = 0.0$. Figure 3 shows the geometric mean for the example motion recorded at Pacoima Dam for four oscillator periods, where the same range of ordinates (a factor of 2) is used for each graph. Also shown is the theoretical result from equation (1), where the ratio has been normalized to equal the observed maximum geometric mean; the theoretical result is shown for $\zeta = 0.0$ and $\zeta = 0.2$. The best agreement between theory and observation is for an oscillator period of 1.0 sec. This is near the period of the large velocity pulse (Fig. 1). The spread of geometric means decreases as the correlation between components decreases. The median of the geometric means over the range of rotation angles is given by the horizontal gray lines. Note that the median is closer to the maximum geometric mean

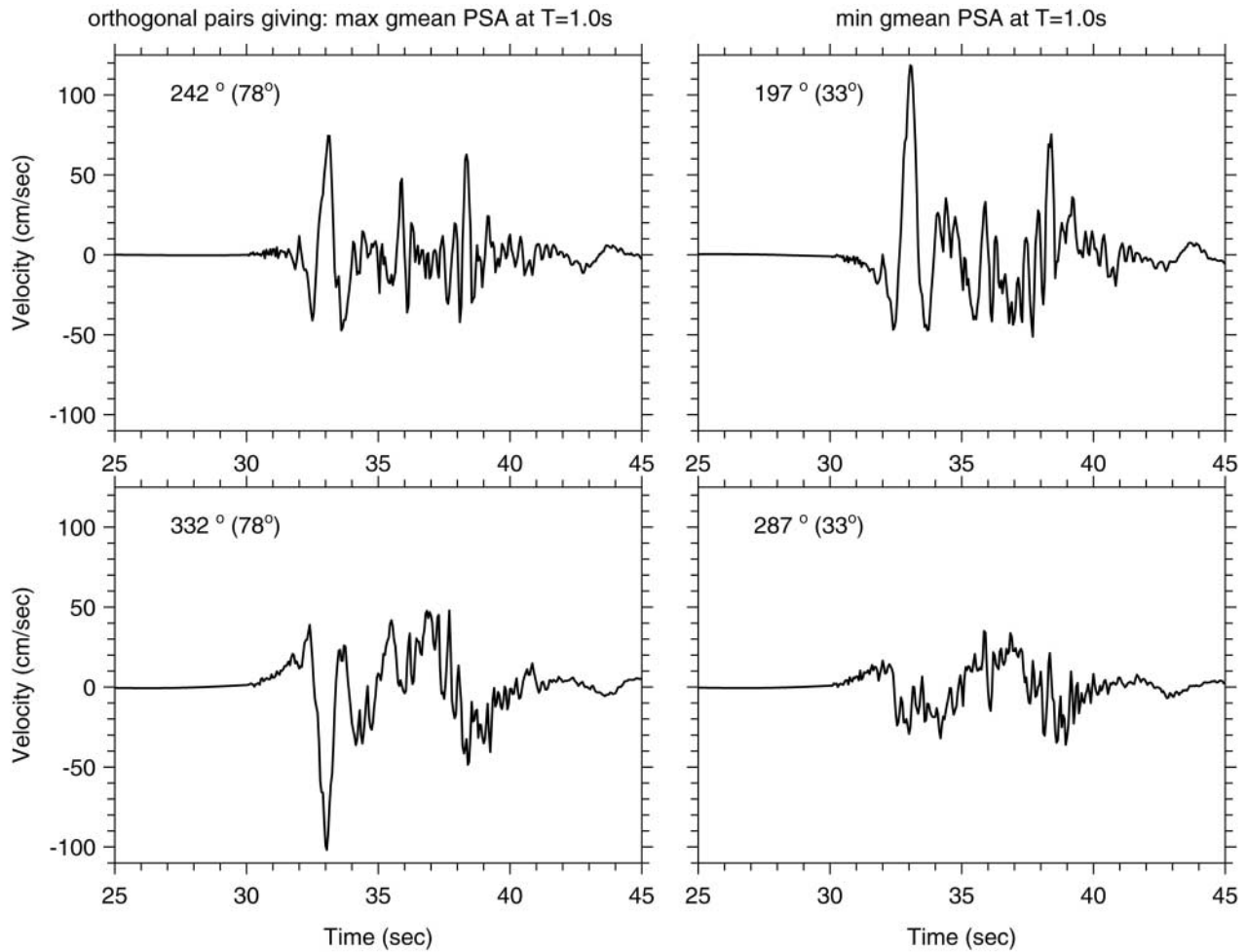


Figure 1. Velocity time series derived from acceleration times series, rotated into an azimuth giving the maximum (left column) and the minimum (right column) geometric-mean response spectra at a period of 1.0 sec. The new sensor orientations are indicated, as are the rotation angles (in parentheses) used to obtain the new orientations. The acceleration records were obtained from Pacoima Dam during the 1971 San Fernando, California, earthquake. The orientations of the original recordings were 164° and 254° . A time-domain acausal low-cut filter with a corner frequency of 0.1 Hz and a low-frequency response going as f^8 was applied to both of the as-recorded acceleration time series before rotation. The time axis includes 30 sec of pre-event zeros added to the time series before filtering (see Boore, 2005b).

than it is to the minimum geometric mean for the $T = 1.0$ sec results. The theoretical results show why this is so: strongly correlated motions will have one rotation angle for which the geometric mean is zero or close to zero, but the minimum is a strong function of the correlation and occurs over a narrow range of rotation angles. The maximum is not a strong function of the correlation between components, and thus any fractile measure of the geometric mean will be closer to the maximum than to the minimum geometric mean.

There is a periodicity of 90° in the geometric means as a function of rotation angles. Because of the periodicity, the nonredundant set of rotation angles spans a range from 0° to 90° . It is easy to see that this is so by considering the defi-

nition of the geometric mean of the response spectra of two horizontal and orthogonal components (call them H_1 and H_2):

$$GM = \sqrt{RS(H_1)RS(H_2)}, \quad (2)$$

where GM is the geometric mean, RS is any type of response spectrum computed for acceleration time series H_i . Rotating the two components by 90° will mean that within a plus or minus sign difference, $H_1 \rightarrow H_2$ and $H_2 \rightarrow H_1$, with the result that GM will be the same (RS is the same for two time series differing only by a 180° phase shift). Because of this periodicity, any fractile of the distribution of geometric means over any set of rotation angles spanning a continuous inter-

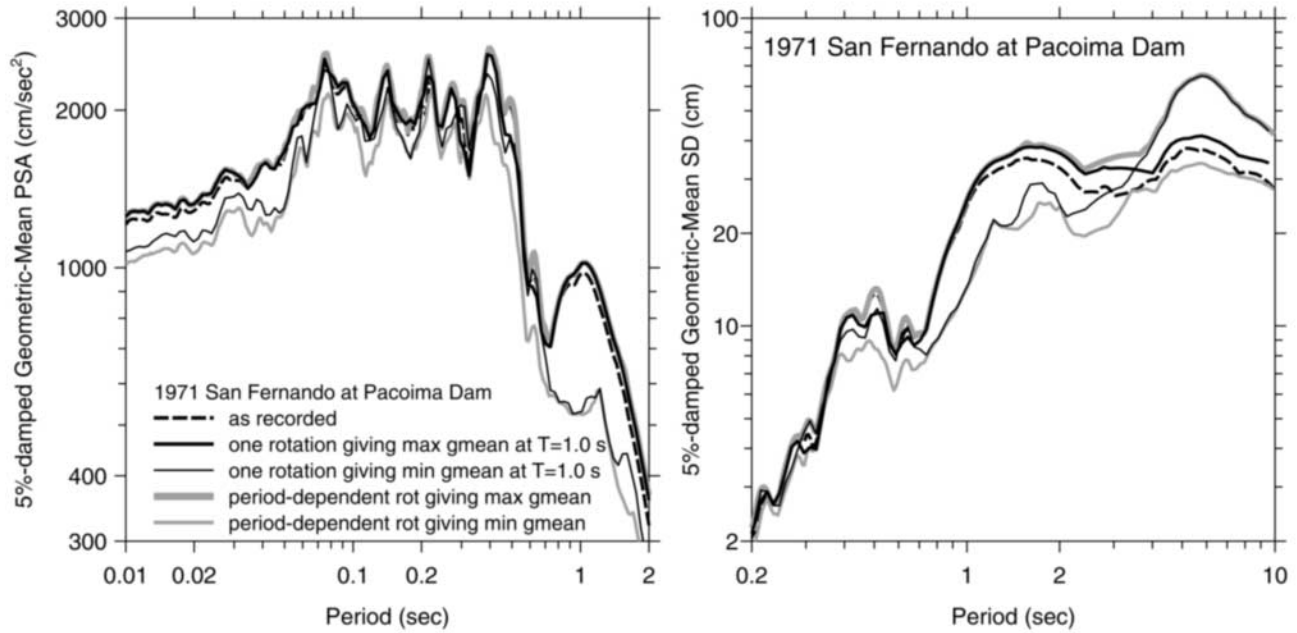


Figure 2. Geometric-mean 5%-damped response spectra for the as-recorded horizontal motions at Pacoima Dam for the 1971 San Fernando earthquake and for various rotations. Spectra are shown for period-independent rotation (rot) angles that minimize and maximize the geometric mean at a period of 1.0 sec. Spectra are also shown for which a different rotation angle is used for each period to minimize and maximize the geometric-mean spectra. Both pseudo-acceleration response spectra (PSA) and displacement response spectra (SD) are shown, to better see the relations between the various measures at short periods and long periods. In the displacement response spectra, note the switch of the single-rotation minimum and maximum geometric mean at periods longer than 3.5 sec.

val of 90° will be the same, which means that such a measure will be independent of the as-recorded orientation of the components. This is the basis for our proposed measures of ground motion, which we expand on in the next section.

GMRotDpp: Orientation-Independent Geometric Mean, Using Period-Dependent Rotation Angles

Motivated by the dependence of the geometric mean on rotation angle, we define new measures of ground motion as a certain percentile value of the set of geometric means obtained using all nonredundant rotations between 0 and 90 degrees. We call these measures GMRotDpp, where “GM” stands for “geometric mean,” “Rot” indicates that rotations over all nonredundant angles are used, “D” indicates that period-dependent rotations are used, and “pp” indicates the percentile value used for the measure (e.g., “00,” “50,” and “100” correspond to minimum, median, and maximum values, respectively; the median value will probably be the commonly used measure, in which case the new measure is GMRotD50). Here is a simple algorithm for computing GMRotDpp.

1. Compute the oscillator time series of each as-recorded horizontal component of motion for the usable range of

oscillator period T_i (the range depends on the processing used to remove noise from the acceleration records). Call these oscillator time series $Osc_1(t, T_i, \eta, 0)$ and $Osc_2(t, T_i, \eta, 0)$, where η is the oscillator damping (we used 5% for the examples in this article), and “0” indicates the rotation angle.

2. Set the rotation angle θ to 0.0.

3. Form the oscillator time series for the rotation angle θ by using linear combinations of the oscillator time series of the as-recorded motions:

$$Osc_1(t, \theta) = Osc_1(t, 0) \times \cos(\theta) + Osc_2(t, 0) \times \sin(\theta) \quad (3a)$$

$$Osc_2(t, \theta) = -Osc_1(t, 0) \times \sin(\theta) + Osc_2(t, 0) \times \cos(\theta), \quad (3b)$$

where for simplicity of notation we have suppressed the arguments T_i and η .

4. Find the largest absolute amplitude of each oscillator time series; these correspond to the response spectral values for period T_i (this is the step that makes the computation of response spectra a nonlinear operation on the time series).

5. Compute the geometric mean as in equation (2) and store

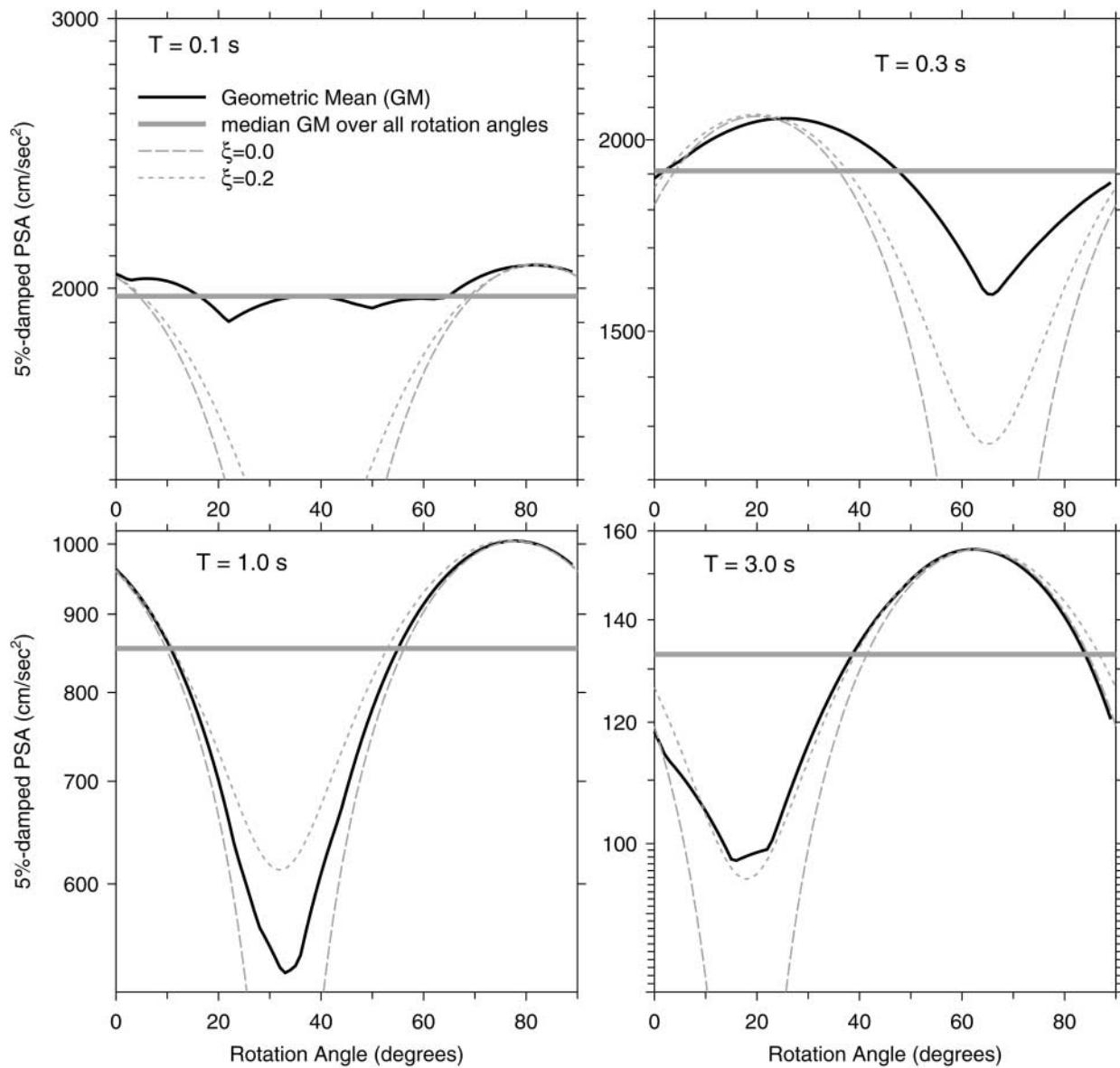


Figure 3. Geometric means of the motions recorded at Pacoima Dam for the 1971 San Fernando earthquake, for four periods, as a function of rotation angle. The horizontal gray line is the 50th-percentile value of the geometric mean, taken over all nonredundant rotation angles ($0-90^\circ$)—we call this GMRotD50. The dashed curves show the predictions based on equation (1), adjusted to have a minimum at the angle corresponding to the minimum of the observed geometric means and a maximum amplitude equal to that of the observed geometric means. Equation (1) is exact only when the motion is linearly polarized (so that ratio of the smaller to larger response spectra ξ on the two horizontal components is 0.0).

in an array giving the geometric mean as a function of rotation angle and period for a fixed value of damping ($GM(\theta, T_i)$).

5. Increment the rotation angle θ by $\Delta\theta$ (we find that a one-degree increment for the rotation angle is sufficient).
6. Repeat steps 3 through 5 until the rotation angle is equal to or greater than 90° .
7. Rank the set corresponding to $GM(\theta, T_i)$ for all values of θ and a fixed value of T_i , from smallest to largest values.
8. Set GMRotD_{pp} to the value of GM corresponding to the specified pp th percentile value. The percentile could be anything (such as the 16th and 84th percentiles), but probably the most commonly used percentile would be 50, which represents the median value (for an even number of rotations we average the sorted values on either side of the midpoint, so with $\Delta\theta = 1^\circ$ there are 90 non-redundant rotations, and the 50th percentile value is calculated as the average of the 45th and 46th ranked val-

ues). GMRotD50 for the example case is shown by the horizontal gray lines in Figure 3. Because of the 90° periodicity, GMRotDpp will be independent of the original orientation of the sensors.

The preceding algorithm requires a program that returns the oscillator response as a time series. If all that is available is a program giving response spectral amplitudes, the algorithm is modified by using the ground-motion acceleration time series rather than the oscillator time series in step 3 and computing response spectral amplitudes of the rotated acceleration time series in step 4. This is somewhat slower than the original algorithm.

GMRotIpp: Orientation-Independent Geometric Mean, Using Period-Independent Rotation Angle

Although the definition of GMRotDpp satisfies our requirement that it is independent of as-recorded sensor orientations, it has the unappealing feature that a single rotation will not produce two time series for which the geometric mean of the individual response spectra equals GMRotDpp for all periods. This is clearly seen in Figure 4, which shows the rotation angles corresponding to GMRotD00 and GMRotD100. The rotation angles in the 0.6-sec to 3-sec period band, roughly the band corresponding to the velocity pulse in Figure 1, show a systematic decrease (perhaps related to the progression of faulting on the rupture surface as well as the distribution of fault slip). Dynamic analysis of structures requires a time series of acceleration, and thus it would be useful to have a ground-motion intensity measure that was not only independent of sensor orientation, but also corresponds to a single rotation of the as-recorded motions. The rotation of the as-recorded motions by this angle would give a single time series of acceleration that has the proper value of the geometric mean. We have devised a scheme to do this, as given in the following steps.

1. Compute GMRotDpp for the usable range of oscillator periods (where the lowest frequency is controlled by the processing required to remove long-period noise).
2. For each oscillator period normalize the set of geometric means for all rotation angles by GMRotDpp for each period. The normalized geometric means for the example case are shown by the gray curves in the upper graph in Figure 5, one curve for each of 200 oscillator periods.
3. Compute the penalty function defined by the equation:

$$\text{penalty}(\theta) = \frac{1}{N_{\text{per}}} \sum_{i=1}^h [GM(\theta, T_i) / \text{GMRotDpp}(T_i) - 1]^2, \quad (4)$$

where the range of usable periods extends from T_l to T_h , $GM(\theta, T_i)$ is the geometric mean of the response spectra for period T_i computed for rotation angle θ , and $\text{GMRotDpp}(T_i)$ is the pp th percentile value of $GM(\theta$,

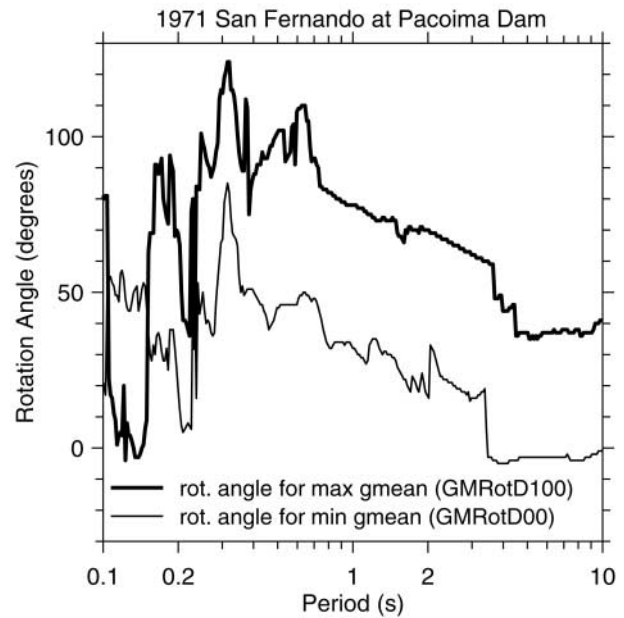


Figure 4. Rotation angle corresponding to the maximum and minimum geometric means; the angle for the 50th percentile geometric mean GMRotD50 will be between the rotation angles shown. (The angles have been “unwrapped,” which is why their range exceeds 90° .)

T_i) over all nonredundant rotation angles, as previously defined (we have only done this computation for $pp = 50$, which we expect to be the most commonly used case, but we, have kept the description general in case there is a need to compute the measure for some other value of pp). This penalty function is shown in the bottom graph of Figure 5 for the example case.

4. Find the rotation angle corresponding to the minimum of the penalty function, θ_{\min} (58° for the example case in Fig. 5).
5. Rotate the as-recorded motions by this angle.
6. Compute the geometric-mean response spectra for the rotated time series. We call the resulting measure of strong motion “GMRotIpp,” where the “I” means that the rotation angle is independent of period. Using the terminology in the equation (4), we have

$$\text{GMRotIpp}(T_i) = GM(\theta_{\min}, T_i). \quad (5)$$

The selection of θ_{\min} seeks to avoid extreme variations away from the desired percentile value over all periods. In particular, for GMRotI50 the procedure avoids the very small geometric means associated with strongly correlated motions. For the example case, the motion on both horizontal components at shorter periods is essentially uncorrelated and the geometric mean shows little azimuthal variation (e.g., Fig. 3 for 0.1 sec). The greatest azimuthal variation in the geometric mean occurs for motion that is strongly polarized (e.g., Fig. 3 for 1.00 sec), and thus it is periods of

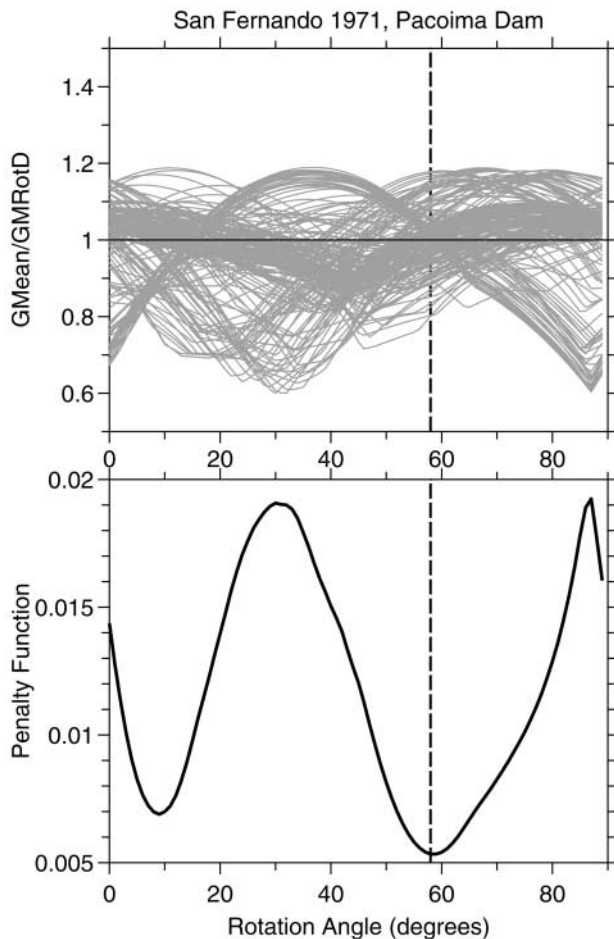


Figure 5. Construction of the GMRotI50 measure of ground-motion intensity. The top graph shows the geometric means for 200 individual periods logarithmically spaced from 0.01 sec to 10.0 sec, normalized by the 50th percentile value for each period (GMRotD50), as a function of rotation angle. The bottom graph shows the penalty function constructed from the 200 normalized geometric means. The minimum of the penalty function gives the period-independent rotation angle (58°, indicated by the vertical dashed line) used to compute the geometric mean that we call “GMRotI50.”

greatest correlation between components that control the value of θ_{\min} . The strong linear polarization tends to occur at moderate to long periods, although the periods at which it occurs can be quite variable (being near 1 sec for the Pacoima Dam recording of the 1971 San Fernando earthquake but periods on the order of 10 sec for other earthquakes, such as the 1999 Hector Mine earthquake [Boore *et al.*, 2002] and the 2003 Bingöl earthquake [Akkar *et al.*, 2005]).

The sensitivity to strongly correlated motions at longer periods can make GMRotIpp dependent on the highest value of period included in the sum defining the penalty function. This is shown in Figures 6 and 7. Figure 6 shows GMRotI50 for four values of T_h : 2.0, 5.0, 6.0, and 20.0 sec. An abrupt change in GMRotI50 takes place for T_h between 5.0 sec and

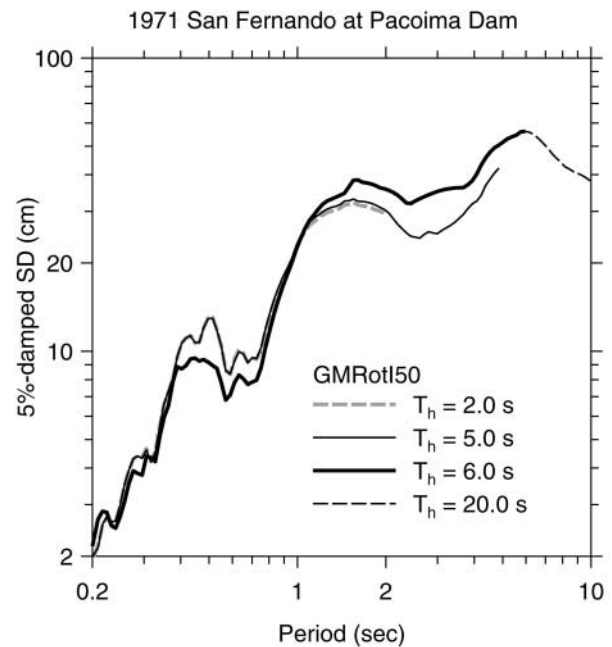


Figure 6. GMRotI50 for 5%-damped oscillators, for various maximum periods (T_h) in the sum defining the penalty function (equation 4). The curves for $T_h = 2.0$ sec and 5.0 sec are almost identical, as are those for $T_h = 6.0$ sec and 20.0 sec.

6.0 sec (the change actually occurs between 5.25 sec and 5.5 sec). The reason for this is related to the relative size of the two minima in the penalty function. The absolute minimum in the penalty switches from the minimum around 58° for T_h of 6 sec and longer to the minimum at 5° for shorter periods. The change takes place abruptly as T_h is decreased from 6 sec to 5 sec. Although not shown here, the rotation angles corresponding to the two minima are quite insensitive to T_h , and thus the values of GMRotI50 are similar for values of T_h either less than or greater than the transition period (Fig. 6). The abrupt change in the relative size of the two minima is related to the large difference in minimum and maximum geometric means for periods around the peak in the displacement response spectrum at 6 sec (see Fig. 2). To avoid the sensitivity of GMRotIpp to T_h , it is important to choose T_h large enough so that all peaks in the displacement response spectrum are included and to have enough values of the oscillator period to define each peak in the response spectrum.

The measures of the geometric mean discussed in this article for $pp = 50$ are shown in Figure 8 for the example case of the Pacoima Dam recording of the 1971 San Fernando earthquake. The measures GMRotD50 and GMRotI50 are similar. As discussed earlier, GMRotD50 is closer to the maximum geometric mean (GMRotD100) than it is to the minimum geometric mean (GMRotD00), in particular for the more strongly correlated longer-period motions.

To study the relation of GMRotI50 to both GMRotD50

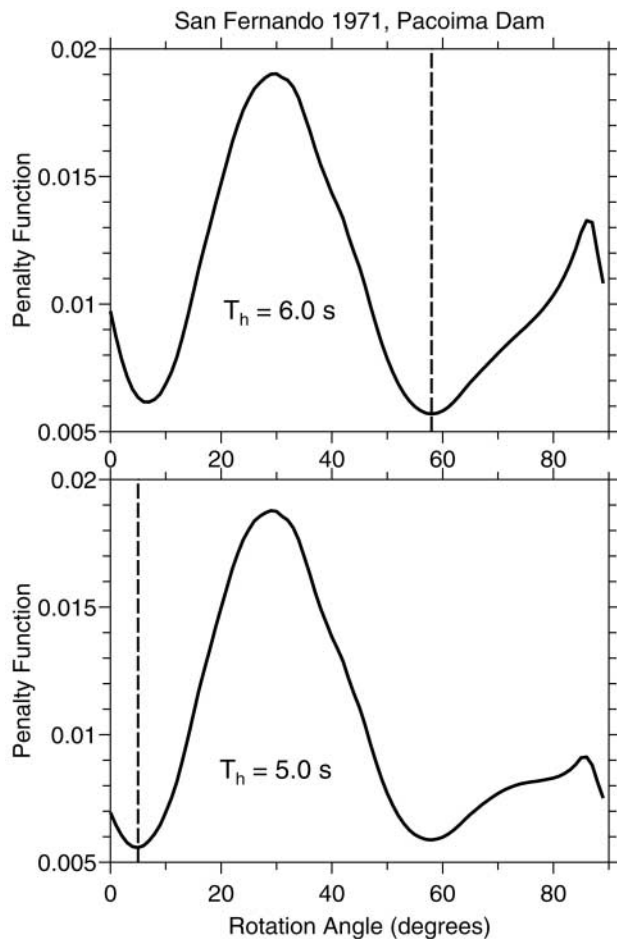


Figure 7. The penalty functions for $T_h = 5.0$ sec and 6.0 sec. The penalty functions were computed for 180 and 186 individual periods logarithmically spaced from 0.01 sec to 5.0 sec and from 0.01 sec to 6.0 sec for $T_h = 5.0$ sec and 6.0 sec, respectively. The vertical dashed lines indicate the rotation angles giving the absolute minimum for each penalty function. These rotation angles were used to compute GMRotI50.

and to the traditional geometric mean from as-recorded motions for more than the one example record, we have computed GMRotD50 and GMRotI50 for more than 3500 records contained in the dataset being used by the PEER NGA project (see the Conclusions section for the web sites describing the project and from which the data can be obtained). For T_h we used the maximum usable oscillator period for each record, as determined from the filters used in processing the data. The natural logarithm of the ratio of GMRotI50 to GMRotD50 has a mean of approximately zero over all periods and a standard deviation less than 0.05 (converted to multiplicative factors, these are shown in Fig. 9). GMRotI50 is systematically higher than the as-recorded ground motion (as shown in Fig. 10), but only by a small amount (less than a factor of 1.03 for the large dataset we studied). The systematic difference is due to the skewed dis-

tribution of the natural logarithm of the geometric mean with respect to rotation angle.

Conclusions and Discussion

We have defined new measures of ground-shaking intensity that combine response spectra for horizontal component recordings in such a way that the measures are independent of the as-installed orientation of the horizontal sensors, the only assumption being orthogonality of the sensors. We define two measures: GMRotD pp , for which the rotation angle required to give the pp th percentile value of all geometric means over the set of nonredundant rotation angles is period dependent, and GMRotI pp , which although requiring GMRotD pp in its computation, corresponds to the geometric-mean response spectra of the two as-recorded horizontal components after a single period-independent rotation of the motions. GMRotI50 has been chosen as the dependent variable in updating the ground-motion prediction equations of Abrahamson and Silva (1997), Boore *et al.* (1997), Campbell and Bozorgnia (2003), and Sadigh *et al.* (1997), as part of a multiyear project sponsored by the Pacific Earthquake Engineering Research Center (the PEER Next Generation Attenuation, [NGA] project—see <http://peer.berkeley.edu/lifelines/nga.html> and <http://peer.berkeley.edu/nga/index.html>). Although no examples are given, GMRotD pp and GMRotI pp with $pp = 16$ and $pp = 84$ might be useful in assessing the variability in response for a given record.

The theoretical advantage of the new measures is that they remove sensor orientation as a contributor to aleatory uncertainty. The main disadvantage is that they require more computation time than the geometric mean of the as-recorded motions (but the computation requirements are not onerous—for the example records used in this article it took 11.7 sec on a 3-GHz PC, without optimization of the compiled Fortran program, to compute GMRotD00, GMRotD50, GMRotD100, and GMRotI50 for 200 oscillator periods). Another possible disadvantage to GMRotD pp is that the period-dependent rotations might seem to obscure the physical interpretation of the measure, a disadvantage not shared by GMRotI pp . On the other hand, in some situations the direction of polarization could change as a function of period, for physical reasons such as rupture propagation along a finite fault or wave arrivals with varying polarizations and frequency content, as might be produced by the distribution of seismic energy into different types of waves and by path complexities that produce lateral refractions. If the polarization angle changes with period (as seems to be the case in the example studied here—see Fig. 4), a single rotation angle might not be appropriate. A possible disadvantage of GMRotI pp is that it requires a choice of a period range for its computation (see equation 4) and care must be taken to make sure that T_h is large enough to capture the peaks in the displacement response spectra.

Whether the reduction in the aleatory uncertainty is of

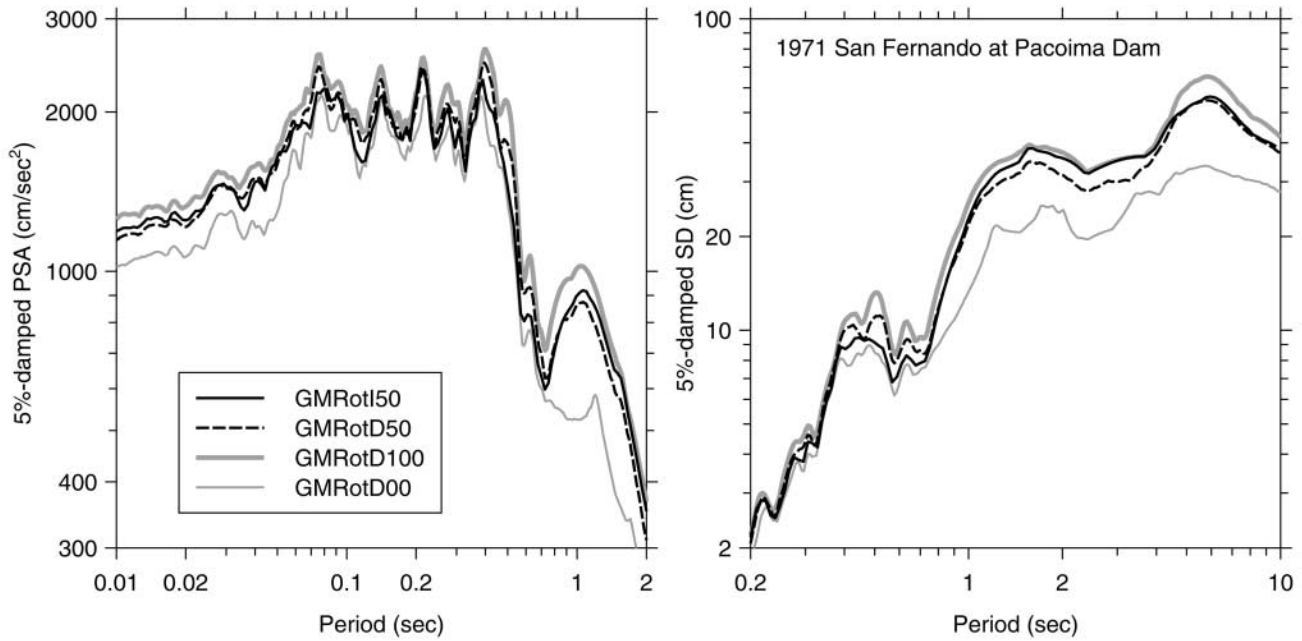


Figure 8. Comparison of GMRotI50 and GMRotD50. Also shown by the gray curves are GMRotD00 and GMRotD100 (the minimum and maximum geometric means using period-dependent rotation angles).

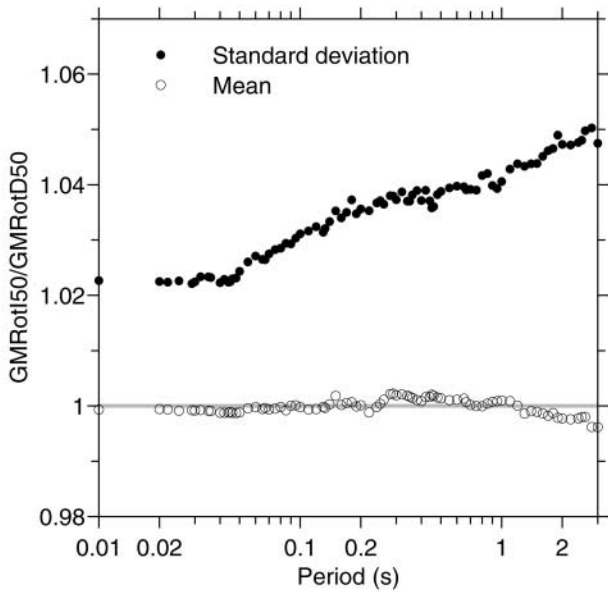


Figure 9. Mean and standard deviation of the natural logarithm of the ratio of GMRotI50 to GMRotD50 for the PEER NGA database, converted to multiplicative factors.

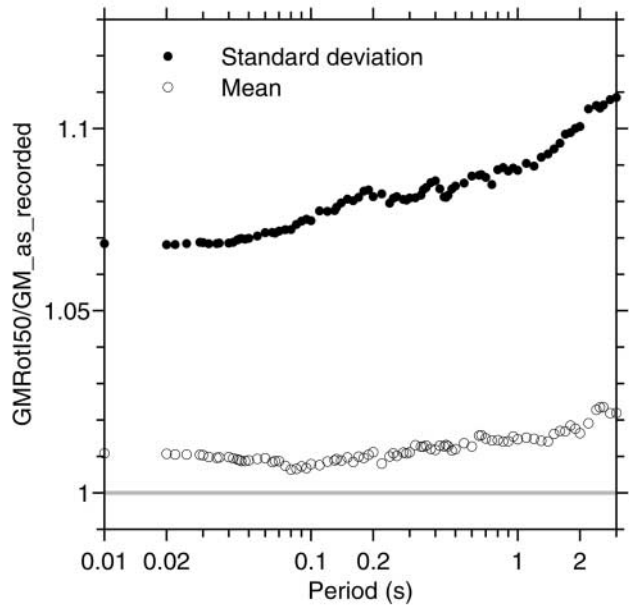


Figure 10. Mean and standard deviation of the natural logarithm of the ratio of GMRotI50 to the geometric-mean response spectra from the as-recorded ground motion for the PEER NGA database, converted to multiplicative factors.

practical significance awaits detailed studies of large datasets. The first such analysis, in the companion paper by Beyer and Bommer (2006), finds for all periods greater than 0.03 sec that the aleatory uncertainty obtained from fitting a simple ground-motion prediction equation to a subset of the PEER NGA dataset is smaller when combining the two hor-

izontal components using GMRotD50 than when using any other procedure for combining the components. The reduction, however, is very small (less than 1%, from figure 7 in Beyer and Bommer), although the reduction does seem to be increasing with increasing period. This period depen-

dence of the reduction suggests that the new measures will be most useful in situations for which strongly correlated motions might be expected (e.g., pulselike motions close to faults). This may be particularly important in deriving correction factors to account for directivity or fault-normal and fault-parallel effects (e.g., Somerville *et al.*, 1997; Abrahamson, 2000; Howard *et al.*, 2005). Assessing this possibility requires analysis of subsets of large databases, as were used by Beyer and Bommer.

Acknowledgments

We thank Paul Spudich for raising awareness of the limitations of as-recorded geometric means and for suggesting a method for speeding up the computation of geometric means for many rotation angles. D.M.B. thanks Jeff Howard for unwittingly motivating him to think about geometric means and rotations. Conversations with Walter Silva and Chris Stephens on the subject were very useful. Detailed reviews by Katrin Beyer, Julian Bommer, Kent Fogleman, Chris Stephens, Fleur Strasser, and an anonymous referee led to substantial improvements of the article.

References

- Abrahamson, N. A. (2000). Effects of rupture directivity on probabilistic seismic hazard analysis, in *Proceedings Sixth International Conference on Seismic Zonation*, Palm Springs, California, 12–15 November 2000, Earthquake Engineering Research Institute.
- Abrahamson, N. A., and K. M. Shedlock (1997). Overview, *Seism. Res. Lett.* **68**, 9–23.
- Abrahamson, N. A., and W. J. Silva (1997). Empirical response spectral attenuation relations for shallow crustal earthquakes, *Seism. Res. Lett.* **68**, 94–127.
- Akkar, S., D. M. Boore, and P. Gülkan (2005). An evaluation of the strong ground motion recorded during the May 1, 2003, Bingöl, Turkey, earthquake, *J. Earthquake Eng. Struct. Dyn.* **9**, 173–197.
- Arias, A. (1970). A measure of earthquake intensity, in *Seismic Design for Nuclear Power Plants*, R. J. Hansen (Editor), The M.I.T. Press, Cambridge, Massachusetts, 438–483.
- Beyer, K., and J. J. Bommer (2006). Relationships between median values and between aleatory variabilities for different definitions of the horizontal component of motion, *Bull. Seism. Soc. Am.* **96**, no. 4, 1512–1522.
- Bommer, J. J., N. A. Abrahamson, F. O. Strasser, A. Pecker, P.-Y. Bard, H. Bungum, F. Cotton, D. Fäh, F. Sabetta, and F. F. Scherbaum (2004). The challenge of defining upper bounds on earthquake ground motions, *Seism. Res. Lett.* **75**, 82–95.
- Boore, D. M. (2005a). Erratum to Equations for estimating horizontal response spectra and peak acceleration from Western North American earthquakes: a summary of recent work, *Seism. Res. Lett.* **76**, 368–369.
- Boore, D. M. (2005b). On pads and filters: processing strong-motion data, *Bull. Seism. Soc. Am.* **95**, 745–750.
- Boore, D. M., W. B. Joyner, and T. E. Fumal (1997). Equations for estimating horizontal response spectra and peak acceleration from western North American earthquakes: a summary of recent work, *Seism. Res. Lett.* **68**, 128–153.
- Boore, D. M., C. D. Stephens, and W. B. Joyner (2002). Comments on baseline correction of digital strong-motion data: examples from the 1999 Hector Mine, California, earthquake, *Bull. Seism. Soc. Am.* **92**, 1543–1560.
- Campbell, K. W., and Y. Bozorgnia (2003). Updated near-source ground-motion (attenuation) relations for the horizontal and vertical components of peak ground acceleration and acceleration response spectra, *Bull. Seism. Soc. Am.* **93**, 314–331.
- Douglas, J. (2003). Earthquake ground motion estimation using strong-motion records: a review of equations for the estimation of peak ground acceleration and response spectral ordinates, *Earth-Sci. Rev.* **61**, 43–104.
- Gonella, J. (1972). A rotary-component method for analysing meteorological and oceanographic vector time series, *Deep-Sea Res.* **19**, 833–846.
- Howard, J. K., C. A. Tracy, and R. G. Burns (2005). Comparing observed and predicted directivity in near-source ground motion, *Earthquake Spectra* **21**, 1063–1092.
- Lu, L., F. Yamazaki, and T. Katayama (1992). Soil amplification based on seismometer array and microtremor observations in Chiba, Japan, *Earthquake Eng. Struct. Dyn.* **21**, 95–108.
- Sadigh, K., C.-Y. Chang, J. A. Egan, F. Makdisi, and R. R. Youngs (1997). Attenuation relationships for shallow crustal earthquakes based on California strong motion data, *Seism. Res. Lett.* **68**, 180–189.
- Shoja-Taheri, J., and B. A. Bolt (1977). A generalized strong-motion accelerogram based on spectral maximization from two horizontal components, *Bull. Seism. Soc. Am.* **67**, 863–876.
- Somerville, P. G., N. F. Smith, R. W. Graves, and N. A. Abrahamson (1997). Modification of empirical strong ground motion attenuation relations to include the amplitude and duration effects of rupture directivity, *Seism. Res. Lett.* **68**, 199–222.
- Spudich, P., B. S. J. Chiou, R. Graves, N. Collins, and P. Somerville (2004). A formulation of directivity for earthquake sources using isochrone theory, *U.S. Geol. Surv. Open-File Rept. 2004-1268*, 54 pp.
- Steidl, J. H. (1993). Variation of site response at the UCSB dense array of portable accelerometers, *Earthquake Spectra* **9**, 289–302.
- Steidl, J. H., A. G. Tumarkin, and R. J. Archuleta (1996). What is a reference site?, *Bull. Seism. Soc. Am.* **86**, 1733–1748.
- U.S. Geological Survey, MS 977
345 Middlefield Road
Menlo Park, California 94025
boore@usgs.gov
(D.M.B.)
- Department of Civil and Environmental Engineering
University of California at Berkeley
Berkeley, California 94720
jenniewl@ce.berkeley.edu
(J.W.-L.)
- Pacific Gas & Electric
245 Market Street
San Francisco, California 94129
naa2@pge.com
(N.A.A.)